Passive scalar cascades in rotating helical and non-helical flows

2013 Phys. Scr. 2013 014037

(http://iopscience.iop.org/1402-4896/2013/T155/014037)

Phys. Scr. **T155** (2013) 014037 (8pp) doi:10.1088/0031-8949/2013/T155/014037

Passive scalar cascades in rotating helical and non-helical flows

P Rodriguez Imazio[1] **and P D Mininni**[1,2]

[1] Departamento de Física, Facultad de Ciencias Exactas y Naturales, Universidad de Buenos Aires and CONICET, Ciudad Universitaria, 1428 Buenos Aires, Argentina
[2] NCAR, PO Box 3000, Boulder, CO 80307-3000, USA

E-mail: paolaimazio@df.uba.ar

Received 25 June 2012
Accepted for publication 24 July 2012
Published 16 July 2013
Online at stacks.iop.org/PhysScr/T155/014037

Abstract
We study how helicity affects the spectrum of a passive scalar in rotating turbulent flows, using numerical simulations of turbulent flows with or without rotation and with or without injection of helicity. Scaling laws for energy and passive scalar spectra in the direction perpendicular to the rotation axis differ in rotating helical flows from those found in the non-helical case, with the spectrum of passive scalar variance in the former case being shallower than in the latter. A simple phenomenological model that links the effects of helicity on the energy spectrum with the passive scalar spectrum is presented.

PACS numbers: 47.32, 47.85

1. Introduction

Enhanced mixing and transport are some of the most important properties of turbulent flows. These properties, sometimes characterized by a turbulent diffusivity, result in rapid homogenization of any mixture of different fluids, are used in many applications [1, 2], and are also relevant in many atmospheric and oceanic flows [3]. In many of these flows, rotation is important, and it is widely accepted that turbulent mixing is affected by the presence of rotation [4–6].

Several studies consider the effect of rotation in the energy cascade. While the energy still undergoes a direct cascade, there is evidence that at moderate rotation rates a fraction of the energy can also undergo an inverse energy cascade, resulting in accumulation of energy at scales larger than the energy injection scale [7, 8]. Nowadays, it is also known that the presence of rotation sets a preferential direction for the transfer of energy in spectral space, with the energy going towards modes with small parallel wavenumber (where parallel is defined relative to the rotation axis) and resulting in a quasi-bidimensionalization of the flow [7, 9, 10]. The energy flux is also reduced (when compared with the homogeneous and isotropic case) by virtue of the extra resonance (or quasi-resonance) condition that triads must fulfill for the coupling between modes to be effective [7, 10]. This results in a steeper energy spectrum than that expected from the Kolmogorov phenomenology. The effect of helicity on rotating turbulence has received less attention, although it is known that helicity is relevant for many atmospheric processes, such as convective thunderstorms [11–13], and is also known to be important for the flows in blood vessels [2]. For the latter case, the results in [14] indicate that helicity affects the energy transfer to smaller scales, making the energy spectrum even steeper than in the rotating non-helical case.

A paradigmatical way to study turbulent mixing is to consider the advection and diffusion of a passive scalar by a turbulent velocity field. When the flow is turbulent, the mixing and transport of a scalar quantity (such as the density of pollutants or aerosols) is greatly enhanced. The turbulent diffusion of a passive scalar in two-point closures is related to the amplitude of the velocity turbulent fluctuations [15], and therefore it can be expected that changes in the scaling law followed by the energy spectrum should affect the dynamics of the passive scalar. The scaling (including intermittency) of passive scalars in isotropic and homogeneous turbulent flows was studied in [16] and later in [1, 17–19]. The Kraichnan model [20] allowed computation of all scaling exponents of the passive scalar for a random, delta-correlated in time velocity field. The predictions are in good agreement with the results of numerical simulations [18], which obtained a joint cascade of energy and passive scalar variance following the same scaling law given by the Kolmogorov spectrum [21], except for intermittency corrections.

Passive scalars in rotating turbulence have also been studied in numerical simulations, showing that the transport

is affected by rotation and anisotropy [22, 23]. Recent numerical studies or rotating turbulence [24] show that passive scalar variance is transferred preferentially toward modes with small parallel wavenumbers (i.e. quasi-bidimensional modes), following an inertial range scaling consistent with the bidimentionalization of the flow. Furthermore, the results show that perpendicular structure functions of the passive scalar have anomalous scaling consistent with the Kraichnan model in a two-dimensional (2D) space, again indicating strong anisotropic mixing and transport of scalar quantities in rotating flows. Experimental evidence for anomalous scaling of passive scalar structure functions in rotating flows was also observed in [25].

Stochastic models and two-point closures indicate that two-particle dispersion in rotating turbulent flows is highly anisotropic, with different dispersion in the direction parallel and perpendicular to the rotation axis [4, 5, 26], which can be related to the diffusion of passive scalars. Numerical simulations [6] also showed that the turbulent diffusivity becomes anisotropic with rotation, reducing the horizontal transport to a much lesser extent than vertical transport.

As in the case of the effect of helicity on the transport and mixing of passive scalars, it was shown in [27] that helicity affects the passive scalar diffusivity in a turbulent flow. For isotropic and homogeneous turbulence, it is argued that the lack of reflectional symmetry (related with a non-zero value of the helicity) produces a turbulent skew-diffusion perpendicular to the local mean scalar gradient. Later, it was shown in [15] using renormalization groups that while anomalous scaling of the passive scalar is not affected by helicity, turbulent diffusion is. However, the effect of helicity on the transport of scalar quantities in rotating helical flows has not been considered.

The aim of this paper is to study how helicity affects the spectrum of a passive scalar in a rotating turbulent flow. The spectrum and flux are studied in numerical simulations of turbulent flows with or without rotation, and with or without injection of helicity, to identify spectral indices in the inertial range of the direct energy and passive scalar cascades. The simulations are performed with a parallel pseudospectral code with periodic boundary conditions [28, 29], using a spatial resolution of 512^3 grid points. The forcing used for all fields is a superposition of random modes, delta-correlated in time, with controllable helicity injection, which in the simulations presented here is either zero or maximal.

Scaling laws for energy and passive scalar spectra in the direction perpendicular to the rotation axis differ in rotating helical flows from those found in the non-helical case. A phenomenological argument that links the effects of helicity on the energy spectrum with the passive scalar spectrum is also presented.

2. Equations and numerical simulations

The data analyzed in the following section is obtained from direct numerical simulations of the incompressible Navier–Stokes equations for the velocity field $\mathbf{u}$ together with the equation for the passive scalar θ, given by

$$\partial_t \mathbf{u} + \mathbf{u}\cdot\nabla\mathbf{u} = -2\boldsymbol{\Omega}\times\mathbf{u} - \nabla p + \nu\nabla^2\mathbf{u} + \mathbf{f}, \tag{1}$$

$$\nabla\cdot\mathbf{u} = 0, \tag{2}$$

$$\partial_t\theta + \mathbf{u}\cdot\nabla\theta = \kappa\nabla^2\theta + \phi, \tag{3}$$

where p is the pressure divided by the (uniform) mass density, ν is the kinematic viscosity and κ is the scalar diffusivity. Here, $\mathbf{f}$ is an external force that drives the turbulence, ϕ is the source of the scalar field and $\boldsymbol{\Omega} = \Omega\hat{z}$ is the rotation.

The numerical code used to solve equations (1)–(3) in a three-dimensional domain of size 2π with periodic boundary conditions is a second-order in time pseudospectral code, parallelized using the Message Passing Interface (MPI) library and OpenMP [28–30]. To solve the pressure, we take the divergence of equation (1), use the incompressibility condition (2) and solve the resulting Poisson equation. To evolve in time a Runge–Kutta method with low storage is used. The code uses the 2/3-rule for de-aliasing, and as a result the maximum resolved wave number is $k_{\max} = N/3$, where $N = 512$ is the linear resolution. All simulations presented are well resolved, in the sense that the dissipation wave numbers k_ν and k_κ (respectively for the kinetic energy and for the passive scalar) are smaller than the maximum wave number $k_{\max}$ at all times.

The dimensionless parameters used to control the simulations are the Reynolds Re, the Peclet Pe and the Rossby Ro numbers, respectively, given by

$$Re = \frac{UL}{\nu}, \tag{4}$$

$$Pe = \frac{UL}{\kappa} \tag{5}$$

and

$$Ro = \frac{U}{2L\Omega}, \tag{6}$$

where U is the rms velocity, and L is the flow forcing scale defined as $L = 2\pi/k_{\rm F}$ with $k_{\rm F}$ the forcing wave number. For most of the simulations shown in the following section $U \approx 2$, and all runs have $\nu = \kappa$ (i.e. $Pe = Re$). The forcing used for the velocity field as well as for the passive scalar is a superposition of Fourier modes with random phases, delta-correlated in time, and the amount of helicity injected is controlled by correlating the velocity field components and the phases between Fourier modes using the method described in [31].

Both the kinetic energy and the passive scalar variance were injected at the same wave number $k_{\rm F}$. One set of runs (set A) has external forcing applied at $k \in [1, 2]$ (therefore $k_{\rm F} \approx 1$, and the simulations have the largest possible separation of scales between the forcing wavenumber and the largest resolved wavenumber). Another set of runs (set B) has forcing at $k \in [2, 3]$ (then $k_{\rm F} \approx 2$). Finally, a third set of runs is forced at $k_{\rm F} = 3$ (set C). For the last set of runs, the choice of $k_{\rm F} = 3$ results in a small separation of scales between the box size and the forcing scale, allowing for some of the energy to be transferred to larger scales in the presence of rotation (although the separation of scales is not large enough to study the inverse cascade). This reduces the Reynolds number and results in a narrower direct cascade inertial range, since the separation between the forcing and the dissipation scale is

Table 1. Parameters used in the simulations: k_F is the forcing wavenumber, Ω the rotation angular velocity, Ro the Rossby number, ν the kinematic viscosity, Re the Reynolds number, U the rms velocity in the turbulent steady state, and $H = \langle \mathbf{u} \cdot \nabla \times \mathbf{u} \rangle$ the total helicity (averaged in time).

Run	k_F	Ω	Ro	ν	Re	U	H
A1	1	0	∞	6×10^{-4}	1000	2	0
A2	1	4	0.04	6×10^{-4}	1000	2	0
B1	2	0	∞	5×10^{-4}	600	2	3
B2	2	8	0.04	5×10^{-4}	600	2	6
B3	2	16	0.04	5×10^{-4}	600	4	11
C1	3	0	∞	6×10^{-4}	240	2	0
C2	3	12	0.04	6×10^{-4}	240	2	0

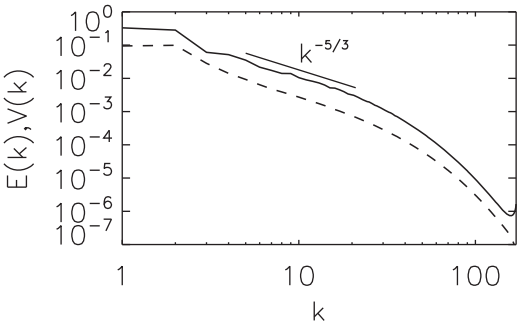

Figure 1. Isotropic energy (solid line) and passive scalar (dashed line) spectrum for run A1 (without rotation and without helicity injection). Kolmogorov scaling is indicated as a reference.

reduced. However, the incipient inverse transfer of energy that develops is important for the development of a dominant direct cascade of helicity when helicity is injected in the presence of rotation (see [14]). The three sets of runs allow us to compare runs with similar Rossby numbers (albeit with different Reynolds numbers) while varying the amount of helicity. While the flows in set B are helical, the flows in sets A and C are non-helical (more details of the runs in sets A and C can be found in [24]).

The simulations were performed as follows: first a simulation of the Navier–Stokes equation with $\Omega = 0$ was done, until a turbulent steady state was reached (this requires an integration for approximately ten turnover times). Then the passive scalar was injected, and the run was continued for another ten turnover times until a steady state for the passive scalar was reached (these runs correspond to runs A1, B1 and C1). Finally, rotation was turned on. Different values of Ω were considered to have similar Rossby numbers in all the runs with $\Omega \neq 0$. All the runs with rotation in each set were started using as initial conditions for the velocity and the passive scalar the latest output of the runs without rotation in the same set (runs A1, B1 or C1, respectively). Each of the runs with rotation was continued for over 20 turnover times. Parameters for all runs are listed in table 1.

3. Numerical results

3.1. Effect of rotation

Figure 1 shows the isotropic energy $E(k)$ and passive scalar variance $V(k)$ spectra for run A1 (without rotation and without helicity injection). An inertial range can be identified,

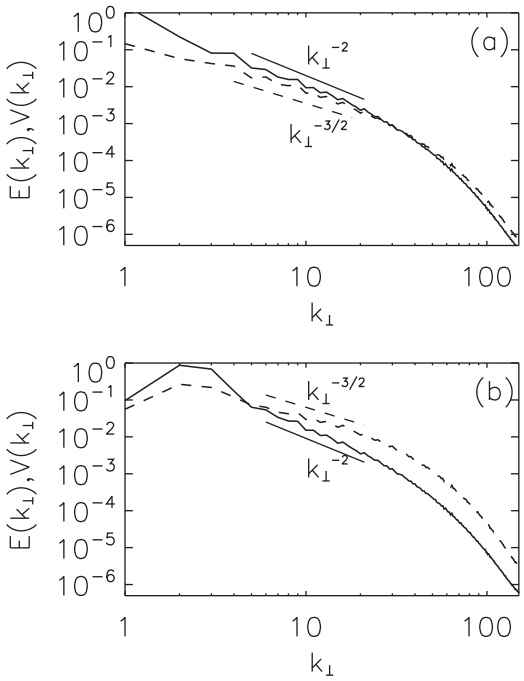

Figure 2. (a) Reduced perpendicular spectrum for the energy (solid line) and for the passive scalar variance (dashed line) for (a) run A2 ($\Omega = 4$) and (b) run C2 ($\Omega = 12$). Scaling laws $\sim k_\perp^{-2}$ and $\sim k_\perp^{-3/2}$ are indicated as references.

where energy and passive scalar follow a $k^{-5/3}$ scaling law, as expected from previous studies of passive scalar in isotropic and homogeneous turbulence [1, 17, 18]. Runs B1 and C1, also without rotation but forced at different wavenumbers (and in the case of run B1, with helicity), show the same scaling.

In figure 2, we show the energy and passive scalar reduced perpendicular spectra, respectively $E(k_\perp)$ and $V(k_\perp)$, for runs A2 and C2 (corresponding to flows with rotation but without net helicity, see table 1). The reduced perpendicular spectrum is obtained by summing over all wavenumbers in Fourier space in cylindrical shells with radius $k_\perp = \sqrt{(k_x^2 + k_y^2)}$, to take into account the fact that the flows become anisotropic in the presence of rotation (see [10, 32] for definitions and details of anisotropic spectra).

As can be seen in figures 2(a) and (b), inertial range scaling can be identified for both the energy and the passive scalar variance, although with different power laws. The reduced perpendicular energy spectrum follows a $\sim k_\perp^{-2}$ scaling. This power law has already been reported in numerical simulations and experiments of rotating turbulence (see, e.g., [14, 33]), and is consistent with simple phenomenological models based on a slowdown of the energy transfer associated with the interaction between waves and eddies [14, 33, 34], as well as with more detailed two-point closures [9, 10]. The passive scalar inertial range displays a scaling compatible with $\sim k_\perp^{-3/2}$ scaling, as also reported in [24]. These power laws can be further confirmed when the spectra are compensated for (see figures 3(a) and (b)). Unlike the case of isotropic and homogeneous turbulence, in the presence of rotation the kinetic energy and passive scalar show different power laws in the inertial range.

The inertial ranges indicated in figures 2 and 3 correspond to direct cascades of energy and scalar variance. This can be

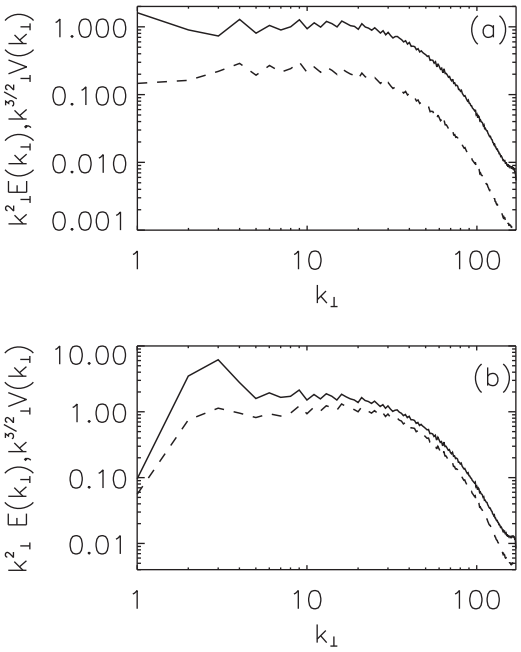

Figure 3. (a) Reduced perpendicular spectrum for the energy (solid line) and for the passive scalar variance (dashed line) compensated for, respectively, by -2 and $-3/2$ in run A2. (b) The same as (a) but for run C2.

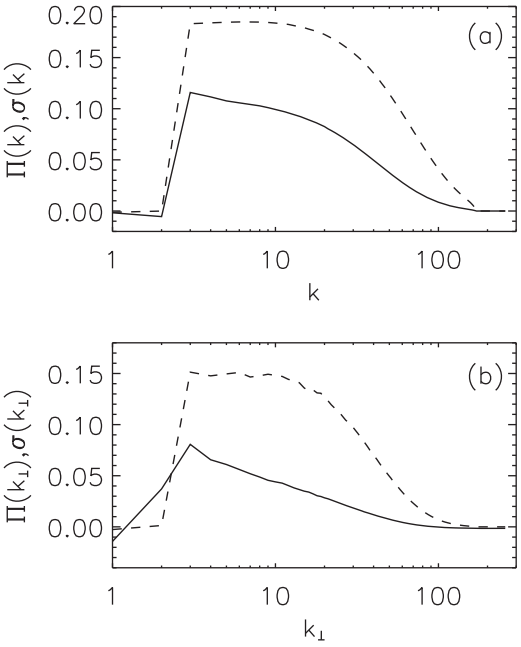

Figure 4. (a) Energy flux $\Pi(k)$ (solid line) and passive scalar flux $\sigma(k)$ (dashed line) for the run without rotation C1. (b) Perpendicular energy flux $\Pi(k_\perp)$ and perpendicular passive scalar flux $\sigma(k_\perp)$ for the run with rotation C2.

confirmed from the energy and passive scalar spectral fluxes shown in figure 4 for runs C1 and C2 (respectively without and with rotation). In the non-rotating case, energy shows a range of approximately constant (and positive) flux, indicating that energy is transferred toward smaller scales, while the energy flux is negligible for wave numbers smaller than the forcing wave number ($k < k_F = 3$). The passive scalar variance also directs cascades to smaller scales with a range of wave numbers with approximately constant flux. When rotation

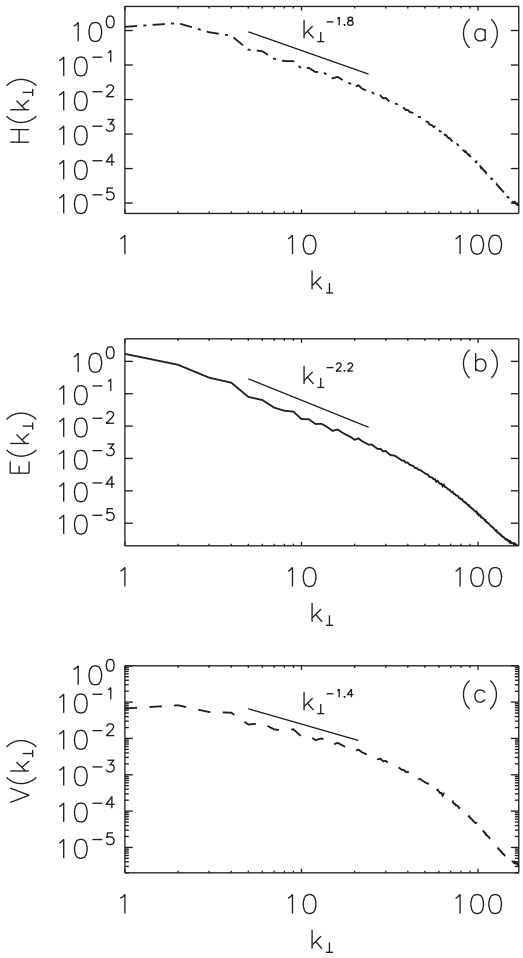

Figure 5. (a) Reduced perpendicular helicity spectrum, (b) energy spectrum and (c) passive scalar spectrum for run B2 (helical turbulent flow with $\Omega = 8$). In all cases slopes are indicated as references.

is present, the energy flux becomes negative for $k < k_F$ (indicating that a fraction of the energy is transferred towards scales larger than the forcing scale, although without enough scale separation to develop an inverse cascade), while the energy flux towards smaller scales remains positive although it decreases when compared with run C1. For the passive scalar, no significative flux toward larger scales is observed, and the cascade remains direct with also a small decrease of the positive (direct) flux for $k > k_F$ when compared with the non-rotating case.

3.2. Effect of helicity

Now we analyze the runs with rotation and with maximal helicity injection, resulting in anisotropic helical turbulent flows. Figures 5 and 6 show the helicity, energy and passive scalar reduced perpendicular spectra for runs B2 and B3. Slopes with reference values for the scaling in the inertial range are also indicated. Whereas without rotation helicity does not change the scaling of the passive scalar spectrum, in the rotating case a difference is observed. A careful analysis of the spectrum indicates that the passive scalar is close to a $\sim k_\perp^{-1.4}$ power law, a spectrum slightly shallower than that observed in runs A2 and C2. The shallower spectrum observed

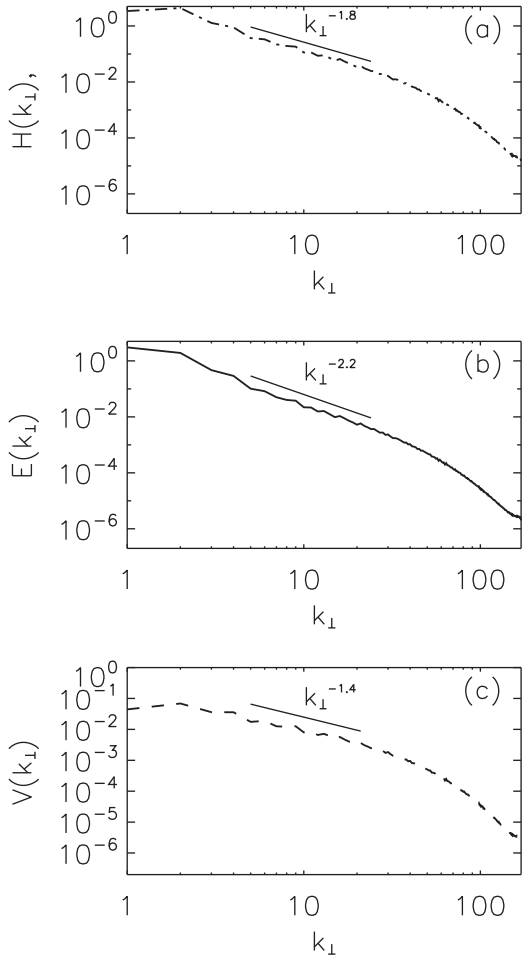

Figure 6. (a) Reduced perpendicular helicity spectrum, (b) energy spectrum and (c) passive scalar spectrum for run B3 (helical turbulent flow with $\Omega = 16$). In all cases slopes are indicated as references.

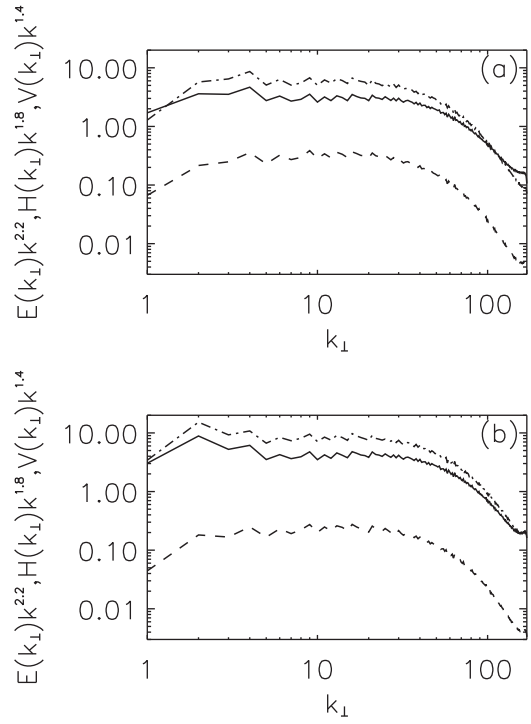

Figure 7. Reduced perpendicular spectra for the helicity (dash-dotted line), energy (solid line), and passive scalar (dashed line) compensated for, respectively, by $k_\perp^{-1.8}$, $k_\perp^{-2.2}$ and $k_\perp^{-1.4}$, in helical runs (a) B2 and (b) B3.

for $V(k_\perp)$ is associated with a change in the energy spectrum when helicity is present.

The energy spectrum in (helical) runs B2 and B3 is steeper than in the (non-helical) runs A2 and C2, as can be also seen in figures 5 and 6. The inertial ranges are compatible with a $\sim k_\perp^{-2.2}$ power law. This result is compatible with the results reported in [14], where numerical simulations were presented showing that in rotating helical flows the direct flux of helicity dominates over the direct flux of energy, affecting the scaling law for the energy in the direct cascade range. A phenomenological argument was also presented, which, assuming that the direct cascade of helicity is dominant, results in a spectrum $E(k_\perp)H(k_\perp) \sim k_\perp^{-4}$. In other words, if the energy spectrum satisfies $E(k) \sim k^{-n}$, then the helicity should scale as $H(k) \sim k^{4-n}$; n becomes larger (and the energy spectrum steeper) as the flow becomes more helical, with the limit $n = 2.5$ for the case of a maximally helical turbulent flow (in practice, this limit cannot be obtained, as a flow with maximal helicity has the nonlinear term in the Navier–Stokes equation equal to zero, and therefore no transfer can take place).

The behavior of the helicity spectrum in runs B2 and B3 is consistent with the phenomenological argument described above. In figures 5 and 6, a scaling $\sim k_\perp^{-1.8}$ is indicated as a reference, which seems compatible with the behavior of $H(k_\perp)$. Compensated spectra for the energy, the helicity and the passive scalar for runs B2 and B3 are shown in figure 7. Good agreement between the reference slopes and the numerical data is apparent.

Following the phenomenological argument mentioned above for the energy spectrum, we can put forward a simple argument to explain the difference observed in the scaling of the passive scalar in rotating helical and non-helical turbulent flows. From equation (3), it can be seen on dimensional grounds that for scales in the inertial range, the passive scalar flux across the scale $l_\perp$ (equal to the passive scalar injection rate) $\sigma = \partial_t \langle \theta^2 \rangle$ must be

$$\sigma \sim \frac{\theta_{l_\perp}^2 u_{l_\perp}}{l_\perp}, \tag{7}$$

where $\theta_{l_\perp}$ is the characteristic concentration of the passive scalar at the scale $l_\perp$, and $u_{l_\perp}$ the characteristic velocity (since the flow becomes anisotropic in the presence of rotation, we are assuming that most of the fluctuations are concentrated in structures with weak variation in the direction along the axis of rotation). If σ is constant in the inertial range, we can estimate the passive scalar spectrum $V(k_\perp) \sim \theta_{l_\perp}^2 / k_\perp$ from equation (7) as

$$V(k_\perp) \sim \frac{\sigma l_\perp^2}{u_{l_\perp}}. \tag{8}$$

If the energy spectrum is $E(k_\perp) \sim k_\perp^{-n}$, and therefore the characteristic velocity at a scale $l_\perp$ is $u_{l_\perp} \sim l_\perp^{1-n}$, the passive scalar spectrum results

$$V(k_\perp) \sim \sigma l_\perp^{\frac{5-n}{2}} \sim \sigma k_\perp^{-\frac{5-n}{2}}. \tag{9}$$

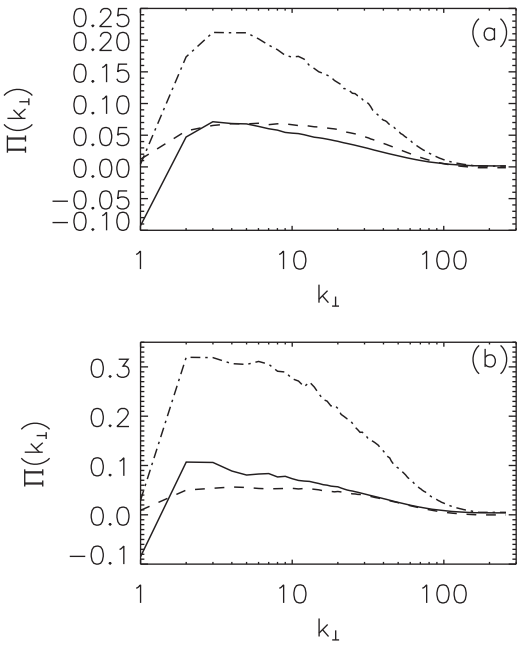

Figure 8. Perpendicular helicity flux $\Sigma(k_\perp)/k_\mathrm{F}$ (dash-dotted line), energy flux $\Pi(k_\perp)$ (solid line) and passive scalar flux $\sigma(k)$ (dashed) for runs (a) B2 and (b) B3.

Therefore, the spectral index for the passive scalar is given by $n_\theta = (5-n)/2$. This result is also valid in the isotropic case, provided that $l_\perp$ is replaced by l.

The numerical results are in good agreement with this simple phenomenological argument. If $n \approx 2$ (runs with rotation but without helicity), then $n_\theta \approx 3/2$. On the other hand, if $n \approx 2.2$ (compatible with the spectrum observed in the runs with rotation and helicity), then $n_\theta \approx 1.4$.

The fact that the fluxes are still positive (i.e. the cascades direct) and approximately constant (within the limitations imposed by the spatial resolution and the moderate Reynolds numbers considered) in rotating helical flows can be confirmed from the helicity, energy and passive scalar fluxes shown in figure 8 for runs B2 and B3 (the helicity flux in the figure is divided by k_F to compare all fluxes with the same units). As in the runs without helicity, the energy flux shows some inverse transfer towards larger scales for $k < k_\mathrm{F}$, while all other fluxes are positive everywhere, indicating that quantities are not transferred towards larger scales. An excess of helicity flux (when compared with the energy flux) can be observed, in agreement with the arguments of dominance of the helicity cascade in [14].

We finish the analysis of the runs by quantifying the degree of anisotropy in the velocity field and in the passive scalar distribution. As already mentioned, the presence of rotation results in a preferred transfer of energy towards 2D modes. This motivated our study of the energy and passive scalar spectral scaling using the reduced perpendicular spectrum instead of the usual isotropic spectrum. We now quantify how much energy and passive scalar variance is in 2D modes in each of the runs. Several anisotropy measures can be used to this end [9, 10, 35]. As an example, the ratio of energy in all modes with $k_\parallel = 0$ to the total energy, i.e. $E(k_\parallel = 0)/E$, can be used to characterize large-scale anisotropy [14]. For a purely 2D flow, this ratio is equal to one. For the passive scalar, the equivalent quantity $V(k_\parallel = 0)/V$ can also be used. Finally, in helical flows we can also compute $H(k_\parallel = 0)/H$ to quantify large-scale anisotropy of the helicity.

As can be seen from table 2, in all the runs a substantial fraction of the energy, the passive scalar variance and (to a lesser extent) the helicity is in 2D modes. Helicity does not seem to affect the large-scale anisotropy. Independently of the helicity in the flow, the energy is more anisotropic at large scales than the passive scalar, as already found for non-helical rotating flows in [24].

To characterize small-scale anisotropy, the Shebalin angles can be used [36, 37]. For the velocity field, the Shebalin angle is defined as

$$\tan^2(\alpha_u) = 2\lim_{l\to 0}\frac{S_2(l_\perp)}{S_2(l_\parallel)} = 2\sum_{k_\perp} k_\perp^2 E(k_\perp)\Big/\sum_{k_\parallel} k_\parallel^2 E(k_\parallel), \tag{10}$$

where $S_2(l_\parallel)$ and $S_2(l_\perp)$ are the second-order longitudinal structure functions of the velocity, respectively with spatial increments in the direction parallel and perpendicular to the axis of rotation. The angle α_u gives a global measure of small scale anisotropy, with a value of $\tan^2(\alpha_u) = 2$ corresponding to an isotropic flow and larger values corresponding to more anisotropic flows. The definition is easily extended to the cases of the passive scalar and the helicity. Table 2 shows the square tangent of the Shebalin angles for the velocity field ($\tan^2(\alpha_u)$), for the passive scalar ($\tan^2(\alpha_\theta)$) and for the helicity ($\tan^2(\alpha_\mathrm{H})$). At the small scales, the flows with helicity seem to develop stronger anisotropies for the passive scalar.

These quantities give information only on the global anisotropy of the velocity field and of the passive scalar. There are other ways to quantify spectral anisotropy that give detailed information on the distribution of energy in spectral space and of the degree of anisotropy at different scales, as the axisymmetric spectrum $e(k_\perp, k_\parallel)$ [10]. A detailed study of spectral anisotropy is left for future work.

4. Concluding remarks

We have presented preliminary results of numerical simulations of passive scalar advection and diffusion in rotating turbulent flows with and without helicity, in grids of 512^3 points.

Whereas in isotropic and homogeneous turbulence at moderate Reynolds number the energy and the passive scalar variance follow Kolmogorov scaling $\sim k^{-5/3}$ except for intermittency corrections, in the presence of rotation non-helical flows display a reduced perpendicular energy spectrum $E(k_\perp) \sim k_\perp^{-2}$ and a shallower reduced perpendicular spectrum $V(k_\perp) \sim k_\perp^{-3/2}$ for the passive scalar.

In the absence of rotation, the scaling of the energy and of the passive scalar remains the same independently of the level of helicity in the flow. In helical rotating flows, our simulations display a steeper energy spectrum compatible with $E(k_\perp) \sim k_\perp^{-2.2}$ and a shallower passive scalar spectrum compatible with $V(k_\perp) \sim k_\perp^{-1.4}$. These numerical results are consistent with a simple phenomenological model that predicts that if the energy spectrum has an inertial range

Table 2. Anisotropy in helical and non-helical runs with rotation. $E(k_\parallel = 0)/E$ is the ratio of energy in all modes with $k_\parallel = 0$ to the total energy, $V(k_\parallel = 0)/V$ is the ratio of scalar variance in modes with $k_\parallel = 0$ to the total scalar variance, and $H(k_\parallel = 0)/H$ is the ratio of helicity in $k_\parallel = 0$ modes to the total helicity. The angles α_u, α_θ and α_H are, respectively, the Shebalin angles for the velocity, the passive scalar and the helicity.

Run	$E(k_\parallel)/E(k)$	$V(k_\parallel)/V(k)$	$H(k_\parallel)/H(k)$	$\tan^2\alpha_u$	$\tan^2\alpha_\theta$	$\tan^2\alpha_H$
A2	0.5	0.4	–	13	20	–
B2	0.6	0.25	0.27	17	37	14
B3	0.4	0.24	0.17	18	76	20
C2	0.2	0.1	–	14	50	–

of the form $E(k_\perp) \sim k_\perp^{-n}$, then the passive scalar spectrum follows a power law $V(k_\perp) \sim k_\perp^{-n_\theta}$ with spectral index $n_\theta = (5-n)/2$.

Finally, analysis of global measures of anisotropy indicate that the distribution of the passive scalar at small scales becomes more anisotropic in helical rotating flows (in comparison with the results in non-helical rotating flows) but it is largely unaffected at large scales.

The results open new questions that will be addressed in future works. In particular, and as the spectral scaling of the passive scalar in rotating flows seems to be affected by helicity, one may ask: is intermittency and anomalous scaling of the passive scalar changed by helicity? And how is the transport and mixing of the passive scalar affected? While the former question can be answered by computing scaling exponents for rotating flows with and without helicity, the latter may require quantification of the turbulent transport in directions parallel and perpendicular to the axis of rotation.

Acknowledgments

PDM acknowledges support from the Carrera del Investigador Científico of CONICET. The authors acknowledge support from grants UBACYT 20020090200692, PICT 2007-02211 and PIP 11220090100825.

References

[1] Falkovich G, Gawedzki K and Vergassola M 2001 Particles and fields in fluid turbulence *Rev. Mod. Phys* **73** 913–74

[2] Morbiducci U, Ponzini R, Rizzo G, Cadioli M, Esposito A, Montevecchi F M and Redaelli A 2011 Mechanistic insight into the physiological relevance of helical blood flow in the human aorta: an *in vivo* study *Biomech. Model. Mechanobiol.* **10** 339–55

[3] Takemi T and Rotunno R 2003 The effects of subgrid model mixing and numerical filtering in simulations of mesoscale cloud systems *Mon. Weather Rev.* **131** 2085–101

[4] Nicolleau F and Vassilicos J C 2000 Turbulent diffusion in stably stratified non-decaying turbulence *J. Fluid Mech.* **410** 123–46

[5] Cambon C, Godeferd F S, Nicolleau F G C A and Vassilicos J C 2004 Turbulent diffusion in rapidly rotating flows with and without stable stratification *J. Fluid Mech.* **499** 231–55

[6] Brandenburg A, Svedin A and Vasil G M 2009 Turbulent diffusion with rotation or magnetic fields *Mon. Not. R. Astron. Soc.* **395** 1599–606

[7] Waleffe F 1992 The nature of triad interactions in homogeneous turbulence *Phys. Fluids* **4** 350

[8] Smith M, Chasnov J and Waleffe F 1996 Crossover from two- to three-dimensional turbulence *Phys. Rev. Lett.* **77** 2468–70

[9] Cambon C and Jacquin L 1989 An approach to non-isotropic turbulence subjected to rotation *J. Fluid Mech.* **202** 295–317

[10] Cambon C, Mansour N N and Godeferd F S 1997 Energy transfer in rotating turbulence *J. Fluid Mech.* **337** 303–32

[11] Lilly D K 1988 The structure, energetics and propagation of rotating convective storms: II. Helicity and storm stabilization *J. Atmos. Sci.* **43** 126–40

[12] Kerr B W and Darkow G L 1996 Storm-relative winds and helicity in the Tornadic thunderstorm environment *Weather Forecast.* **11** 489–505

[13] Markowsky P M, Straka E N, Rasmussen E N and Blanchard D O 1998 Variability of storm-relative helicity during VORTEX *Mon. Weather Rev.* **126** 2959–71

[14] Mininni P D and Pouquet A 2009 Helicity cascades in rotating turbulence *Phys. Rev.* E **79** 026304

[15] Chkhetiani O G, Hnatich M, Jurcisinova A, Jurcisin M, Mazzino A and Repasan M 2006 The influence of helicity on scaling regimes in the extended Kraichnan model *J. Phys. A: Math. Gen.* **39** 7913–26

[16] Kraichnan R 1968 Small scale structure of a scalar field convected by turbulence *Phys. Fluids* **11** 945

[17] Sreenivasan K R 1991 On local isotropy of passive scalars in turbulent shear flows *Proc. R. Soc. Lond.* A **434** 165–82

[18] Chen S and Kraichnan R 1998 Simulations of a randomly advected passive scalar field *Phys. Fluids* **10** 2867–84

[19] Warhaft Z 2000 Passive scalars in turbulent flows *Annu. Rev. Fluid. Mech.* **32** 203–40

[20] Kraichnan R 1994 Anomalous scaling of a randomly advected passive scalar *Phys. Rev. Lett.* **72** 1016–9

[21] Kolmogorov A N 1941 The local structure of turbulence in incompressible viscous fluid for very large Reynolds number *Dokl. Akad. Nauk SSSR* **30** 301–5

[22] Yeung P K and Xu J 2004 Effects of rotation on turbulent mixing: nonpremixed passive scalars *Phys. Fluids* **16** 93–103

[23] Brethouwer G 2005 The effect of rotation on rapidly sheared homogeneous turbulence and passive scalar transport. Linear theory and direct numerical simulation *J. Fluid Mech.* **542** 305–42

[24] Rodriguez Imazio P and Mininni P 2011 Anomalous scaling of passive scalars in rotating flows *Phys. Rev.* E **83** 066309

[25] Moisy F, Willaime H, Andersen J S and Tabeling P 2001 Passive scalar intermittency in low temperature helium flows *Phys. Rev. Lett.* **86** 4827–30

[26] Kimura Y and Herring J R 1997 Particle dispersion in rotating stratified turbulence *APS Division of Fluid Dynamics Meeting abstract* #Fh.04

[27] Moffat H K 1983 Transport effects associated with turbulence with particular attention to the influence of helicity *Rep. Prog. Phys* **46** 621–64

[28] Gómez D O, Mininni P D and Dmitruk P 2005 MHD simulations and astrophysical applications *Adv. Space Res.* **35** 899–907

[29] Gómez D O, Mininni P D and Dmitruk P 2005 Parallel simulations in turbulent MHD *Phys. Scr.* **T116** 123–7

[30] Mininni P D, Rosenberg D, Reddy R and Pouquet A 2011 A hybrid MPI-OpenMP scheme for scalable parallel pseudospectral computations for fluid turbulence *Parallel Comput.* **37** 316–26

[31] Pouquet A and Patterson G S 1978 Numerical simulation of helical magnetohydrodynamic turbulence *J. Fluid Mech.* **85** 305–23
[32] Mininni P D, Rosenberg D and Pouquet A 2012 Isotropization at small scales of rotating helically driven turbulence *J. Fluid Mech.* **699** 263–79
[33] Müller W C and Thiele M 2007 Scaling and energy transfer in rotating turbulence *Europhys. Lett.* **77** 34003
[34] Zhou Y 1995 A phenomenological treatment of rotating turbulence *Phys. Fluids* **7** 2092
[35] Bartello P, Métais O and Lesieur M 1994 Coherent structures in rotating three dimensional turbulence *J. Fluid Mech.* **542** 1–29
[36] Shebalin J V, Mattheus W H and Montgomery D 1983 Anisotropy in MHD turbulence due to a mean magnetic field *J. Plasma Phys.* **29** 525–47
[37] Milano L J, Matthaeus W H, Dimitruk P and Montgomery D C 2001 Local anisotropy in incompressible magnetohydrodynamic turbulence *Phys. Plasmas* **8** 2673